

# Fluence to Effective Dose Conversion Coefficients for Electrons from 1MeV to 100GeV

S. Tsuda, A. Endo, Y. Yamaguchi and O. Sato<sup>1</sup>

*Department of Health Physics, Japan Atomic Energy Research Institute  
Tokai, Ibaraki 319-1195, Japan*

<sup>1</sup>*Mitsubishi Research Institute, INC.  
Otemachi, Chiyoda-ku, Tokyo 100-8141, Japan*

## Abstract

Fluence to effective dose conversion coefficients have been calculated for electrons from 1MeV to 100GeV using an anthropomorphic phantom and the EGS4 code. The conversion coefficients were calculated for typical six different irradiation geometries by taking electro-magnetic cascade shower and photonuclear reaction into account. The contribution due to photonuclear reaction in energies up to 140MeV was evaluated to be less than 0.2% to absorbed dose.

## 1 Introduction

Dose limits are expressed in terms of the quantities, introduced in the Recommendation of the International Commission on Radiological Protection (ICRP). The effective dose, in ICRP publication 60 (ICRP60) [1], is defined as the sum of risk-weighted organ doses and used as a radiological protection quantity related to total stochastic effect on human body. Since this quantity is not measurable in practice, the conversion coefficient, calculated for standard conditions of exposure from physical quantities such as particle fluence to effective dose, has been used for the external radiation protection. ICRP has compiled the conversion coefficients against external radiations such as photons up to 10MeV, neutrons up to 180MeV and electrons up to 10MeV in ICRP Publication 74 (ICRP74) [2]. However, there has been growing need of dose conversion coefficients for higher energy or various kinds of radiation.

After the publication of ICRP74, the conversion coefficients have been calculated by several groups for photons [3, 4] up to 10GeV and for neutrons [5, 6], protons [6, 7], muons [8] and pions [9] up to 10TeV. As for fluence to effective dose conversion coefficients for electrons up to GeV order, Ferrari et al. [10] calculated the conversion coefficients for electrons up to 10GeV in four different types of geometries using FLUKA [11], the Monte Carlo high energy radiation transport code. The conversion coefficients for higher energy electrons will be needed for the radiation protection in synchrotron electron facilities etc.

In the present study, fluence to effective dose conversion coefficients were calculated for electrons in an energy range from 1MeV to 100GeV, using an anthropomorphic phantom and the photon electron Monte Carlo simulation code EGS4 [13]. The calculations have included the evaluation of both electro-magnetic process and photonuclear reaction, which are caused by high-energy bremsstrahlung produced in a human body. In the calculation of effective dose due to photonuclear reaction, the reactions such as  $(\gamma, p)$ ,  $(\gamma, d)$ ,  $(\gamma, t)$ ,  $(\gamma, {}^3\text{He})$ ,  $(\gamma, \alpha)$  and  $(\gamma, n)$  were considered. The contribution of photonuclear reaction to absorbed dose was also evaluated.

## 2 Method of Calculation

### 2.1 Effective dose

In ICRP60, effective dose is defined as

$$E = \sum_T w_T H_T, \quad (1)$$

where  $w_T$  is the tissue weighting factor for tissue or organ, T, and  $H_T$  is the equivalent dose in tissue or organ, T. The tissue weighting factors are given for 12 tissues or organs and remainder including 10 tissues or organs.  $H_T$  is given by

$$H_T = \sum_R w_R D_{T,R}, \quad (2)$$

where  $w_R$  is the radiation weighting factor for radiation R and  $D_{T,R}$  is the absorbed dose for tissue or organ, T, due to radiation R. For photons and electrons,  $w_R$  is assigned to be unity. When it comes to the treatment of colon, we treated the lower large intestine as colon and the upper large intestine as one of the remainder tissues, according to ICRP60.

In the evaluation of electro-magnetic process,  $D_{T,R}$  was obtained by dividing deposited energy in each organ or tissue by its own mass.

In the case of photonuclear reaction, using the averaged photon fluence in each organ or tissue calculated by EGS4, absorbed dose for charged particles were calculated by

$$D_i = \frac{1}{\rho} \sum_j \int_{E_i} E_i \int_{E_\gamma} N_j \cdot \sigma_{ij}(E_\gamma) \cdot f_j(E_i, E_\gamma) \cdot \bar{\phi}(E_\gamma) dE_\gamma dE_i, \quad (3)$$

where

- $D_i$  : absorbed dose for charged particle  $i$ , such as proton (p), deuteron (d), triton (t),  $^3\text{He}$ , and  $\alpha$ -particle ( $\alpha$ ),
- $\rho$  : density of organs or tissue,
- $E_i$  : energy of charged particle  $i$ ,
- $E_\gamma$  : photon energy,
- $N_j$  : atom number density of  $j$ -nucleus such as C, N, O,
- $\sigma_{ij}(E_\gamma)$  : cross section of  $j$ -nucleus for  $i$ -particle production when photon energy is  $E_\gamma$ ,
- $f_j(E_i, E_\gamma)$  : energy spectrum of secondary particle  $i$  by the reaction between photon and  $j$ -nucleus,
- $\bar{\phi}(E_\gamma)$  : averaged photon fluence in organs or tissue.

In this calculation, it is assumed that recoiled nuclei and secondary charged particles deposit their whole energies on the spot of each organ or tissue where the particles are produced (kerma approximation). However, we did not evaluate the contribution of secondary neutrons because of the following reasons. The first is that the contribution of neutron to absorbed dose will be overestimated under the assumption of the kerma approximation. The second is, that it is reported the contribution of neutron produced to absorbed dose is considerably small [14] when a 30cm-thick semi-infinite slab phantom are irradiated by photons in the energy range up to 10GeV.

As for recoiled nuclei, the kinetic energy,  $E_i^{Recoil}$ , was calculated by energy conservation law and dose equivalents were obtained by substituting  $E_i^{Recoil}$  for  $E_i$  in Eq.(3). Total absorbed dose was composed of those due to electro-magnetic cascade shower and photonuclear reaction.  $H_T$  in each organ or tissue was converted from the total absorbed dose in Eq.(2). Finally, we obtained  $E$  by summing the product of  $H_T$  for the organs or tissues and  $w_T$  in Eq.(1).

### 2.2 Photonuclear cross section

Photonuclear cross sections of secondary particle production were taken from preliminary version of JENDL Photonuclear Data Files (JENDL-PDF) [18]. We treated the main elements in a human

body such as carbon, nitrogen and oxygen. The reaction types included were  $(\gamma, p)$ ,  $(\gamma, d)$ ,  $(\gamma, t)$ ,  $(\gamma, {}^3\text{He})$ ,  $(\gamma, \alpha)$  and  $(\gamma, n)$ . The cross sections of the six reactions including the giant dipole resonance peaks were given for the photon energy up to 140MeV. The photonuclear reaction was evaluated for the components of photon fluence with energy below 140MeV.

### 2.3 Mathematical phantom and Monte Carlo code

An anthropomorphic phantom and EGS4 were used to calculate energy deposition and photon fluence averaged over each tissue or organ. The mathematical phantom used in the calculation was a modified MIRD-type phantom, in which oesophagus was added by Yamaguchi [15]. The phantom [15] is designed as hermaphroditic and composed of the 61 regions, or 37 organs and tissues with different densities and composition. Three tissues have been considered: soft tissues, lungs and skeletal tissue. The density assumed is  $0.9869 \text{ g}\cdot\text{cm}^{-3}$  for soft tissues,  $0.2958 \text{ g}\cdot\text{cm}^{-3}$  for lungs and  $1.4682 \text{ g}\cdot\text{cm}^{-3}$  for skeletal tissue. The composition of the three tissues were limited to the 17 elements, H, C, N, O, Na, Mg, P, S, Cl, K, Ca, Fe, Zn, Rb, Sr, Zr, Pb.

To incorporate the phantom into the EGS4 code system, UCGEN [16], the generalized user code for EGS4, was used. The user code employs modified MARS geometry package [17] developed at ORNL, and the MIRD-type anthropomorphic phantom was described with this geometry package.

The phantom was irradiated in a vacuum space by mono-energetic parallel electron beams. Selected irradiation geometries were anterior-posterior (AP), posterior-anterior (PA), right lateral (RLAT), left lateral (LLAT), isotropic (ISO) and rotational (ROT).

Cut off energies for photons and electrons were set to be 10keV and 100keV respectively since the range for electrons with the cut off energies is short as compared with the tissue or organ size in the phantom. Histories were selected to keep the statistical uncertainties below 10% for equivalent doses of organ or tissue that were given the tissue weighting factors.

## 3 Results and Discussion

### 3.1 Dose contribution due to photonuclear reaction

The contribution of photonuclear reaction to absorbed dose is expressed by the ratio of absorbed doses due to photonuclear reaction against the total absorbed dose, as shown in Fig.1. In AP irradiation geometry, the maximum contribution of photonuclear reaction to the total absorbed dose is about 0.1%. The predominant reactions were  $(\gamma, n)$  and  $(\gamma, p)$  reactions, due to the large cross sections compared with other reactions. The contribution of photonuclear reaction to doses gradually increases with incident electron energy up to about 500MeV and then changes little up to 100GeV. As for other irradiation geometries, the each energy dependence of the ratio was similar to that in AP geometry and the maximum contributions to absorbed dose are within 0.2%.

In the present evaluation, the doses in the photon energy range above 140MeV were neglected because of the lack of the cross section in JENDL-PDF. According to Sato et al. [14], the cross sections above 140MeV are comparable or greater than the cross section at the energy of giant dipole resonance peaks. In the case of the incident electron energy 100GeV in AP geometry, the ratio of photon fluences above 140MeV up to 100GeV amounted to more than 50% and the contribution of photon fluence above 140MeV was estimated to be over 50%. Then the contribution of photonuclear reactions to absorbed doses has been underestimated. However, the contribution of photonuclear reaction to absorbed dose was estimated to be within 1% and considerably small against total absorbed doses, even if the absorbed doses in energies over 140MeV were considered.

### 3.2 Dose conversion coefficients

Fluence to effective dose conversion coefficients are summarized and compared with Ferrari's data [10] in Table 1. Statistical uncertainties (fractional standard deviation) are presented for each

value. The same data are also plotted in Fig.2. In the coefficients, both electro-magnetic cascade process and photonuclear reaction were considered.

As shown in Fig.2, the coefficients sharply increase with incident electron energy up to 50MeV, while those for electron energies over 50MeV increase gradually. The type of geometry with the maximum  $E$  is dependent on incident electron energies. In the energy range below 50MeV, the  $E$  values are higher for AP than for any other geometries. This is because the range of electron is short and most of electron energies are deposited in the area near the surface of the phantom, where organs or tissues with large  $w_T$  such as testes and breast are located. At 50MeV, significant difference in the  $E$  values was not found among irradiation geometries. The reason is that the range of electron with 50MeV is estimated to be about 16 cm and nearly equal to the thickness of the phantom. For electron energy over 100MeV, the  $E$  values for RLAT or ISO become the maximum. The range of electron becomes larger and energy deposition increases in organs or tissues located inside and on the rear of the phantom against its incident direction. The variation of organ dose conversion coefficients decreases with incident electron energy in the energy range over 50MeV.

For LAT geometry, there are some difference in  $E$  between for right lateral (RLAT) and for left lateral (LLAT). This result can be explained by the position of specific organs, such as stomach and colon, with high tissue weighting factor.  $E$  is about 10% higher for RLAT than for LLAT in the energy range over 50MeV, mainly because stomach and colon, with relatively high  $w_T$ , were located at the left side of phantom. The  $E$  values for ROT resulted in nearly averaged values for AP, PA and LAT geometry.

The data are in a good agreement with Ferrari's data in the energy range up to 100MeV. In AP, the results show agreement within 6% in the energy range over 20MeV. In other irradiation geometries, there is no significant difference as well. As a result, the conversion coefficients calculated for the energy range over 10MeV are valid data. On the other hand, some of the present results in the energy range below 10MeV exceed by about 40% those of the reference data. These discrepancies might be attributed to the difference in phantom, compared the calculated organ doses with Ferrari's data.

The data calculated in the present study will contribute a determination of the dose limit for electrons.

## 4 Conclusion

Effective dose per unit fluence for electrons has been calculated from 1MeV to 100GeV using the photon-electron Monte Carlo simulation code, EGS4, combined with an anthropomorphic phantom. Photonuclear reaction has been also considered in the conversion coefficient below photon energy 140MeV. The calculated conversion coefficients are generally in agreement with those up to 100GeV calculated by FLUKA. The dose contributions of photonuclear reaction to absorbed dose were estimated to be less than 0.2% in any irradiation geometries and found to be not so significant even if the cross section of photonuclear reaction above 140MeV were considered. We will provide a complete dataset of fluence to effective dose conversion coefficients for electrons up to 100GeV.

## References

- [1] International Commission on Radiological Protection, "1990 Recommendations of the International Commission on Radiological Protection", *ICRP Publication 60. Ann. ICRP 21* (1-3) (1991).
- [2] International Commission on Radiological Protection, "Conversion Coefficients for use in Radiological Protection against External Radiation", *ICRP Publication 74, Ann. ICRP26* (3/4) (1998).

- [3] Sato, O., Iwai, S., Tanaka, S., Uehara, T., Sakamoto, Y., Yoshizawa, N. and Furihata, S. ,  
“Calculation of Equivalent Dose and Effective Dose Conversion Coefficients for Photons from  
1MeV to 10GeV”, *Radiat. Prot. Dosim.* **62**(1995)119-130.
- [4] Ferrari, A., Pelliccioni, M. and Pillon, M., “Fluence to Effective Dose and Effective Dose Conversion  
Coefficients for Photons from 50keV to 10GeV”, *Radiat. Prot. Dosim.* **67**(1996)245-251.
- [5] Ferrari, A., Pelliccioni, M. and Pillon, M., “Fluence to Effective Dose Conversion Coefficients for  
Neutrons up to 10TeV”, *Radiat. Prot. Dosim.* **71**(1997)165-173.
- [6] Yoshizawa, N., Sato, O., Takagi, S., Furihata, S., Iwai, S., Uehara, T., Tanaka, S. and Sakamoto,  
Y., “External Radiation Conversion Coefficients using Radiation Weighting Factors and Quality  
Factors for Neutron and Proton from 20MeV to 10GeV”, *Nucl. Sci. Tech.* **35**(12)(1998)928-942.
- [7] Ferrari, A., Pelliccioni, M. and Pillon, M., “Fluence to Effective Dose Conversion Coefficients for  
Protons from 5MeV to 10TeV”, *Radiat. Prot. Dosim.* **71**(2) (1997)85-91.
- [8] Ferrari, A., Pelliccioni, M. and Pillon, M., “Fluence-to-Effective Dose Conversion Coefficients for  
Muons”, *Radiat. Prot. Dosim.* **74**(4)(1997)227-233.
- [9] Ferrari, A., Pelliccioni, M. and Pillon, M., “Fluence to Effective Dose Conversion Coefficients for  
Negatively and Positively Charged Pions”, *Radiat. Prot. Dosim.* **80**(4)(1998)361-370.
- [10] Ferrari, A., Pelliccioni, M. and Pillon, M., “Fluence to Effective Dose and Effective Dose  
Equivalent Conversion Coefficients for Electrons from 5MeV to 10GeV”, *Radiat. Prot. Dosim.*  
**69**(2)(1997)97-104.
- [11] Aarnio, P. A., Fasso, A., Ferrari, A., Möhring, J. -H., Ranft, J., Sala, P. R., Stevenson, G. R. and  
Zazula, J. M., “FLUKA: Hadronic Benchmarks and Applications”, In: Proc. MC93 Int. Conf. on  
Monte Carlo Simulation in High Energy and Nuclear Physics, Tallahassee, 22-26 February 1993  
(Ed. World Scientific) (1994).
- [12] Ranft, J. and Nelson, W. R., “Hadron Cascades Induced by Electron and Photon Beams in the  
GeV Energy Range”, *Nucl. Instrum. Methods.* **A257**(1987)177-184.
- [13] Nelson, W. R., Hirayama, H. and Rogers, W. O., “The EGS-4 Code System”, *SLAC-265* (1985).
- [14] Sato, O., Yoshizawa, N., Iwai, S., Uehara, T., Sakamoto, Y. and Tanaka, S., *J. Nucl. Sci. Tech.*  
*supplement 1*(2000)861-864.
- [15] Yamaguchi, Y., “Dose Conversion Coefficients for External Photons Based on ICRP 1990 Rec-  
ommendations”, *J. Nucl. Sci. Tech.* **31**(1994)716-725.
- [16] Momose, T., Nojiri, I., Narita, O., Iwai, S., Rintsu, Y., Sato, O. and Nakamura, M., “improve-  
ment in the EGS4 code system - General Purpose Electron-Photon Monte Carlo Transport Code  
System”, In: Proc. The first EGS4 User’s Meeting in Japan, 48-73 (1990).
- [17] West, J. T. and Emmett, M. B., “MARS: A Multiple Array System Using Combinatorial Geom-  
etry”, *NUREG/CR-0200*, vol.3, sect.M9 (1993).
- [18] Fukahori, T. private communication.

Table 1. Fluence to Effective dose conversion coefficients.

(pSv·cm <sup>2</sup> )																
Energy (MeV)	AP				PA				ISO				RLAT			
	Present work		Ferrari et al.		Present work		Ferrari et al.		Present work		Ferrari et al.		Present work		Ferrari et al.	
1	365	0.6 %			1.94	1.6 %			2.08	0.3 %			2.25	1.3 %		
5	77.3	0.8 %	71.9	3.0 %	13.6	1.4 %	7.4	1.9 %	32.9	0.8 %	20.7	4.3 %	8.91	1.6 %	8.95	3.2 %
10	131	0.7 %	152	1.7 %	40.1	1.3 %	42.7	1.1 %	57.1	0.4 %	51.2	4.3 %	21.3	1.3 %	20.5	2.3 %
20	243	0.9 %	248	1.8 %	114	1.1 %	124	2.4 %	101	0.7 %	112	4.7 %	69.5	1.3 %	81.1	1.8 %
30	312	1.0 %	299	1.9 %	230	0.6 %	264	3.2 %	161	0.8 %	163	4.6 %	115	1.4 %	136	2.0 %
50	339	1.2 %	337	2.6 %	340	0.7 %	341	2.8 %	243	0.9 %	245	3.2 %	210	1.4 %	230	2.0 %
100	353	0.8 %	358	3.3 %	367	0.8 %	364	1.9 %	329	0.8 %	328	3.4 %	324	1.0 %	329	2.5 %
200	360	0.9 %	366	3.2 %	382	0.8 %	384	2.8 %	384	0.6 %	377	3.8 %	395	0.9 %	407	4.0 %
500	368	1.1 %	389	2.8 %	400	1.2 %	415	2.4 %	454	1.4 %	453	4.0 %	460	1.0 %	468	2.9 %
1,000	383	1.5 %	399	3.6 %	429	0.9 %	418	2.3 %	501	1.4 %	506	3.5 %	518	1.0 %	509	3.7 %
5,000	407	1.1 %	416	3.5 %	473	1.0 %	468	2.4 %	650	1.0 %	648	3.7 %	652	1.3 %	634	4.1 %
10,000	414	1.3 %	430	2.7 %	485	1.3 %	491	3.0 %	725	1.1 %	739	3.5 %	703	1.5 %	721	3.5 %
50,000	438	1.4 %			535	1.3 %			913	1.1 %			862	1.2 %		
100,000	448	0.9 %			571	1.7 %			1039	1.0 %			933	1.0 %		

Energy (MeV)	LLAT		ROT	
	Present work		Present work	
1	1.17	0.7 %	7.15	0.6 %
5	9.33	0.5 %	28.7	1.0 %
10	21.7	0.9 %	60.6	0.6 %
20	63.6	0.9 %	133	0.7 %
30	126	0.9 %	209	0.7 %
50	236	0.9 %	295	1.1 %
100	339	0.9 %	353	1.0 %
200	395	0.9 %	385	1.0 %
500	463	1.2 %	419	1.1 %
1000	495	1.2 %	446	1.4 %
5000	602	1.3 %	507	1.1 %
10000	661	1.4 %	537	1.6 %
50000	795	1.2 %	630	1.6 %
100000	846	1.1 %	653	1.2 %

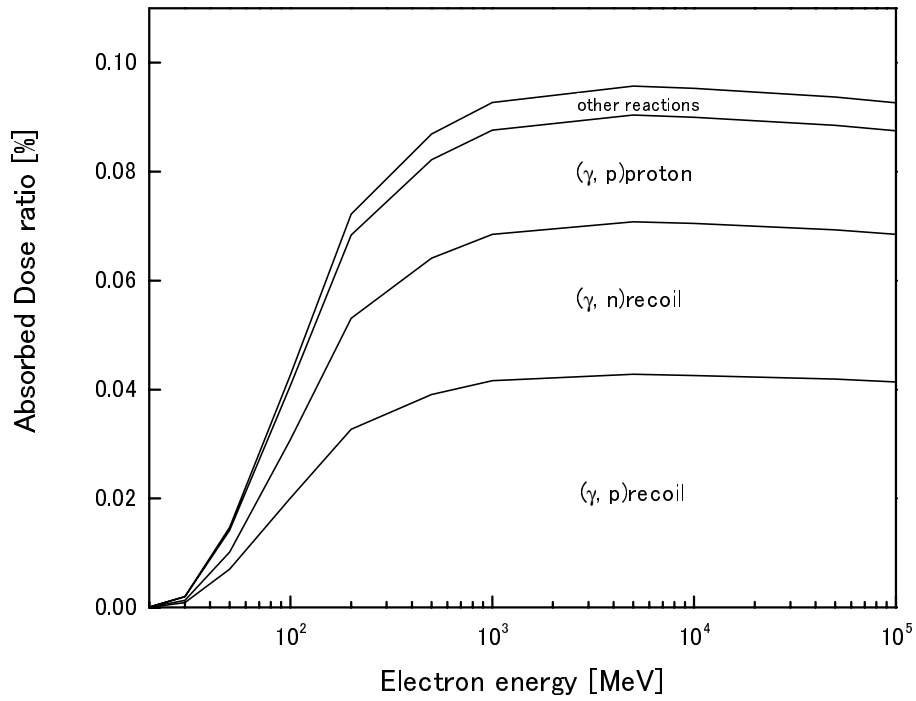


Figure 1. The ratio of absorbed dose by photonuclear reaction to total dose equivalent in AP geometry. Others include secondaries and recoiled charged particles produced by the reactions such as  $(\gamma, d)$ ,  $(\gamma, t)$ ,  $(\gamma, {}^3\text{He})$ ,  $(\gamma, \alpha)$  and  $(\gamma, n)$ .

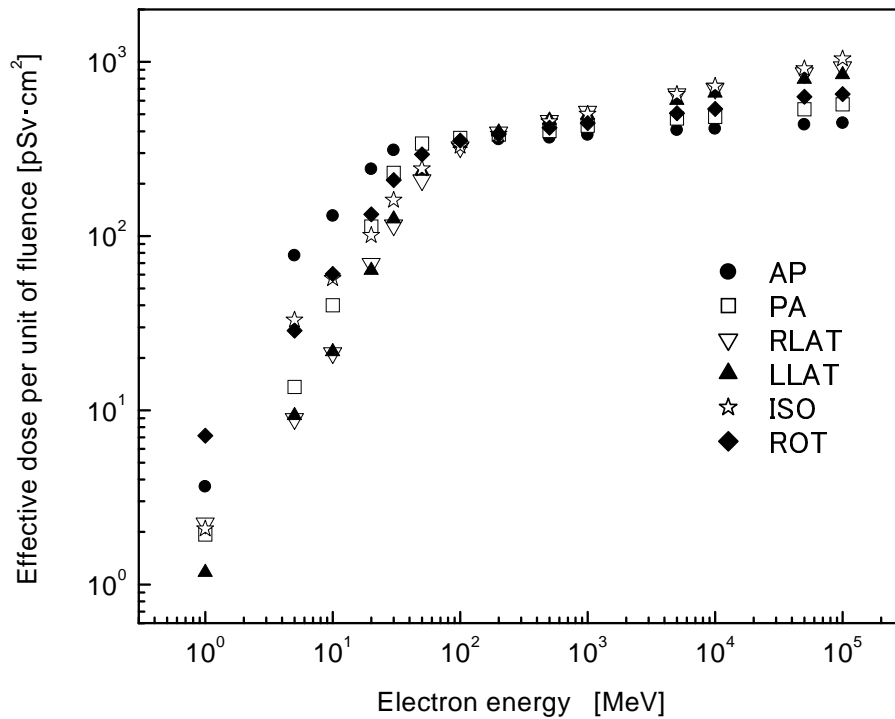


Figure 2. Effective dose per unit fluence as a function of incident electron energy.